

CCAAT/Enhancer-binding Protein β DNA Binding Is Auto-inhibited by Multiple Elements That Also Mediate Association with p300/CREB-binding Protein (CBP)* \dagger

Received for publication, March 31, 2010, and in revised form, April 29, 2010. Published, JBC Papers in Press, May 7, 2010, DOI 10.1074/jbc.M110.128413

Sook Lee[‡], Maria Miller[§], Jon D. Shuman^{†1}, and Peter F. Johnson^{‡2}

From the [‡]Laboratory of Cancer Prevention and [§]Macromolecular Crystallography Laboratory, NCI-Frederick, National Institutes of Health, Frederick, Maryland 21702-1201

Signaling through Ras GTPases controls the activity of many transcription factors including CCAAT/enhancer-binding protein (C/EBP β), which regulates oncogenic H-Ras^{V12}-induced senescence and growth arrest. Here we report that C/EBP β (LAP) DNA binding is inhibited by N-terminal sequences and derepressed by oncogenic Ras signaling. Sequence and mutational analyses showed that auto-repression involves two LXXLF (ϕ XX $\phi\phi$)-like motifs (LX1 and LX2) and a third element, auto-inhibitory domain (AID), located within conserved region CR5. LX1 is a critical component of the transactivation domain and has been shown to mediate C/EBP β binding to the TAZ2 region of p300/CREB-binding protein coactivators. C/EBP β auto-repression also involves a C-terminal regulatory domain (CRD) adjacent to the leucine zipper. CRD contains a third ϕ XX $\phi\phi$ motif (LX3) and a short sequence, KQL, which has similarity to a region in the protein-binding site of TAZ2. The C/EBP β N- and C-terminal domains physically associate in a manner that requires the basic region and CRD. We propose a model in which the regulatory sequences form a hydrophobic core that reciprocally inhibits DNA binding and transactivation. We also suggest a mechanism for C/EBP β derepression involving several recently identified modifications within AID and CRD. Finally, we show that association of activated C/EBP β with p300/CREB-binding protein requires the LX2 and AID auto-inhibitory elements. Thus, the N-terminal regulatory elements have dual roles in auto-inhibition and coactivator binding.

Post-translational regulation of transcription factors (TFs)³ is a common means of controlling gene expression in response to extrinsic and intrinsic cellular signals (1). Several activities of

TFs, including DNA binding, dimerization, transactivation, subcellular localization, and protein stability, can be influenced by signal-dependent modifications. For example, the association of CREB with its coactivator p300/CBP requires phosphorylation on Ser-133 (2), and phosphorylation of steroid receptors regulates their DNA binding and transactivation functions (3). Stimulus-induced increases in DNA binding have been observed for several TFs, suggesting that their binding activity is intrinsically repressed (auto-inhibited) in the absence of an activating signal (4). Auto-inhibition serves as a mechanism to stringently control the activity of proteins involved in critical biological processes such as signal transduction, proliferation, development, and tumorigenesis. In some cases, specific auto-inhibitory sequences have been identified. For instance, Graves and colleagues (5) have shown that Ets-1 DNA binding is repressed by inhibitory regions flanking the DNA-binding domain.

Tumor cells frequently contain activating mutations in Ras GTPases, growth factor receptors that signal through Ras, or downstream kinases such as Raf. These dysregulated signals are ultimately transmitted to TFs such as AP-1 that alter gene expression and promote oncogenic transformation (6). C/EBP β is a member of the CCAAT/enhancer-binding protein family of bZIP TFs (7) that has emerged as another physiological target of Ras signaling. C/EBP β can mediate either pro-oncogenic or anti-oncogenic responses to activated Ras, depending on the cellular context (8). The pro-oncogenic functions of C/EBP β include suppression of apoptosis (9), which in some cases has been shown to involve regulation of the growth and survival factor, IGF-1 (10). In contrast, C/EBP β has an anti-oncogenic role in primary fibroblasts where it promotes oncogene-induced senescence (11, 12). Oncogene-induced senescence is a permanent state of cell cycle arrest induced by oncogenic stress, such as expression of constitutively activated forms of Ras and Raf, and provides a barrier to tumor development (13). Oncogene-induced senescence is bypassed in *Cebpb*^{-/-} mouse embryonic fibroblasts (11) and in human diploid fibroblasts lacking C/EBP β (12), demonstrating the importance of C/EBP β in cell cycle arrest and senescence.

In view of the key role C/EBP β plays in cellular responses to oncogenic and physiological Ras signals, we wish to understand the pathways and mechanisms that control its activity. We and others (14, 15) previously showed that C/EBP β is an intrinsically repressed protein that contains two regions, termed regulatory domains 1 and 2 (RD1 and RD2), which inhibit transac-

* This work was supported by the Intramural Research Program of the National Institutes of Health, National Cancer Institute, Center for Cancer Research.

\dagger This article was selected as a Paper of the Week.

¹ Present address: Brewton-Parker College, Mount Vernon, GA 30445.

² To whom correspondence should be addressed: Bldg. 539, Rm. 122, NCI-Frederick, National Institutes of Health, Frederick, MD 21702-1201. Fax: 301-846-5991; E-mail: johnsope@mail.nih.gov.

³ The abbreviations used are: TF, transcription factor; C/EBP, CCAAT/enhancer-binding protein; EMSA, electrophoretic mobility shift assay; bZIP, basic region-leucine zipper; DBD, DNA-binding domain; BR, basic region; LZ, leucine zipper; TAD, transactivation domain; RD, regulatory domain; CRD, C-terminal regulatory domain; TLS, TAZ2-like sequence; CBP, CREB-binding protein; CREB, cAMP-response element-binding protein; AID, auto-inhibitory domain; HA, hemagglutinin; GST, glutathione S-transferase; WT, wild type; ERK, extracellular signal-regulated kinase; RSK, ribosomal S6 kinase; MEK, mitogen-activated protein kinase/ERK kinase; aa, amino acids; m, mutant; LAP, liver-enriched transcriptional activator protein; LIP, liver-enriched inhibitory protein.

C/EBP β Auto-inhibition

tivation. RD1 includes a conserved SUMOylation site that influences the transcriptional activity of several C/EBP family members (15). Leutz and colleagues (16, 17) also reported that two phylogenetically conserved regions in chicken C/EBP β (aka NF-M), CR5 and CR7, inhibit transactivation of a reporter gene and suppress NF-M-mediated activation of endogenous myelomonocytic-specific target genes. Auto-inhibition was overcome by expression of kinase oncogenes such as *ras*, *raf*, or *v-erbB*, indicating that oncogenic signals stimulate the transcriptional functions of C/EBP β .

Here we have extended these observations by showing that C/EBP β DNA binding is intrinsically repressed and becomes activated by oncogenic Ras signaling (see also Ref. 18). We identified three short sequences in the N-terminal portion of C/EBP β that mediate auto-inhibition: a region of high hydrophobicity and predicted secondary structure termed the "auto-inhibitory domain" (AID) that resides within CR5 and two ϕ XX ϕ ϕ -like motifs (ϕ denotes a hydrophobic residue). ϕ XX ϕ ϕ or LXXLL/LXXLF motifs are α -helical sequences involved in inter- and intraprotein interactions and that are critical for auto-inhibition of steroid receptors and other regulatory proteins (19, 20). A third ϕ XX ϕ ϕ motif was identified near the C/EBP β C terminus, which is also involved in auto-repression. We propose that intramolecular interactions involving these motifs and the bZIP region maintain C/EBP β in a repressed state that inhibits both DNA binding and transactivation. We further show that the three N-terminal auto-inhibitory elements mediate association of C/EBP β with p300/CBP coactivators.

EXPERIMENTAL PROCEDURES

Plasmid Constructs—The G₅E1b-luc reporter, pcDNA3.1 expression vectors for rat C/EBP β , and GAL4-C/EBP β constructs have been described (21). pcDNA3-H-Ras^{V12} was obtained from C. Der. The 2 \times C/EBP-Luc reporter was a gift from P. Rorth (Carnegie Institution of Washington) and contains two repeats of the consensus C/EBP-binding site, 5'-TGC-AGATTGCGCAATCTGCA-3', upstream of the minimal thymidine kinase promoter (22). C/EBP β LXXLF motif mutants (mLX1, mLX2, and mLX3) and other point mutants were generated by site-directed mutagenesis (Stratagene). Serial C-terminal deletions (STOP mutants) were generated by placing a termination codon at each repeated leucine position in the leucine zipper. pcDNA3-CBP₁₆₈₀₋₂₄₄₁-2 \times FLAG (23) was kindly provided by J.-R. Cardinaux. p300 constructs were obtained from Addgene: pCMVb-HA-p300 (Addgene ID 10718; W. Sellers) and TAZ2 mutant d33 (24) (Addgene ID 10719).

Cell Transfection and Preparation of Lysates—HEK293T cells were maintained in Dulbecco's modified Eagle's medium with 10% fetal bovine serum. 1.5×10^5 cells were cultured in 60-mm plates for 24 h and transfected with 500 ng of pcDNA3.1-C/EBP β without or with 100 ng of H-Ras^{V12} plasmid using 2 μ l of FuGENE (Roche Applied Science) per μ g of DNA. After transfection, cells were cultured in complete medium for 24 h and serum-starved overnight prior to harvest, and nuclear extracts were prepared for electrophoretic mobility shift assay (EMSA). C/EBP β levels were analyzed by immuno-

blotting using antibody C-19 (Santa Cruz Biotechnology). For transactivation assays, cells were transfected with 100 ng of 2 \times C/EBP-luc or G₅E1b-luc reporter plasmid and 10 ng of C/EBP β or GAL4-C/EBP β vector, without or with 10 ng of Ras^{V12} plasmid. Where appropriate, 50 ng of pCMVb-HA-p300 was included. After overnight starvation, cells were lysed in 1 \times passive lysis buffer, and lysates were analyzed using the luciferase assay system (Promega). Luciferase activity was normalized to total protein in the lysates.

EMSAs—The EMSA probe was a double-stranded oligonucleotide containing a consensus C/EBP-binding site (underlined) (5'-GATCCATATCCCTGATTGCGCAATAGGCTCAAAA-3') labeled with [γ -³²P]ATP and T4 polynucleotide kinase. The probe was incubated with nuclear extract in a 25- μ l reaction containing 20 mM HEPES, pH 7.5, 200 mM NaCl, 5% Ficoll, 5 mM dithiothreitol, 5 mM EDTA, 1 μ g of poly[d(I-C)], 1 μ g of bovine serum albumin, and 4 μ l of radioimmune precipitation buffer at room temperature for 30 min. DNA-protein complexes were separated on 6% polyacrylamide/1 \times Tris-bo- rate-EDTA gels.

Recombinant Proteins—His-tagged C/EBP β constructs containing a tobacco etch virus cleavage site after the His₆ tag (25) were cloned using Gateway recombination technology (Invitrogen). After isopropyl-1-thio- β -D-galactopyranoside induction in *Escherichia coli*, cells were collected and resuspended in lysis buffer (20 mM Tris-HCl, pH 6.8, 150 mM NaCl, 1 mM EDTA, 1 mM benzamidine, 0.2 mM phenylmethylsulfonyl fluoride, 1 μ g/ml antipain, 0.1% β -mercaptoethanol, 0.5% Nonidet P-40) containing 50 μ g/ml lysozyme. After mild sonication and centrifugation, the pellet containing insoluble C/EBP β was resuspended in solubilization buffer (5 M urea, 50 mM Tris-HCl, pH 8.0, 0.1% β -mercaptoethanol, 1 mM benzamidine, 0.2 mM phenylmethylsulfonyl fluoride, 5 μ g/ml antipain) and rotated overnight. The solubilized protein was clarified and bound to a nickel-nitrilotriacetic acid column (Promega). The column was washed serially with solubilization and washing buffer (5 M urea, 50 mM Tris-HCl, pH 8.0, 0.1% β -mercaptoethanol, 5 mM imidazole, 5 μ g/ml antipain). Protein was eluted with 50 mM Tris-HCl, pH 6.5, 0.3 M NaCl, 0.1% β -mercaptoethanol, 0.5 M imidazole and dialyzed against 50 mM Tris-HCl, pH 8.0, 0.3 M NaCl, 0.1% β -mercaptoethanol, 50 mM imidazole, with 0.5 M arginine included to prevent aggregation. 25 μ g/ml purified tobacco etch virus protease (25) was added to the dialyzed eluate and incubated overnight at room temperature, after which the sample was applied to a nickel-nitrilotriacetic acid column three times to remove the His₆ fragment. Tobacco etch virus-cleaved C/EBP β in the flow-through fraction was dialyzed against 50 mM Tris-HCl, pH 8.0, 200 mM NaCl, 5% glycerol, 1 mM dithiothreitol for 2 h at room temperature, applied to a MonoS fast protein liquid chromatography column, and eluted using a linear NaCl gradient. N-terminal C/EBP β fragments 22–104 and 22–192 were prepared similarly except that MonoQ chromatography was used for the final purification step and the dialysis/loading buffer contained 10 mM NaCl.

GST Fusion Proteins and Pulldown Assays—The Gateway recombination system was used for cloning of GST fusion proteins. Isopropyl-1-thio- β -D-galactopyranoside-induced bacterial cell pellet was resuspended in 10 mM Tris-HCl, pH 8.0, 150

mM NaCl, 1 mM EDTA with protease inhibitors and incubated with 100 μ g/ml lysozyme for 15 min on ice. After adding 5 mM dithiothreitol and 1.5% sarcosyl(*N*-lauroylsarcosine), the lysate was sonicated for 1 min (six pulses for 10 s with a 20-s rest). After adding Triton X-100 to a final concentration of 2–4%, the solubilized GST protein was immobilized on glutathione-agarose beads (BD Biosciences). For pull-down assays, GST or GST·DBD beads (normalized for the amount of GST protein) were incubated with purified C/EBP β N-terminal fragments (22–104 or 22–192) in binding buffer (20 mM HEPES, pH 7.5, 50 mM KCl, 20 μ M ZnSO₄, 10% glycerol, and 0.1% Triton X-100) at room temperature for 2 h. After washing six times with binding buffer, the bound material was eluted in sample buffer, separated by 16% SDS-PAGE, and transferred to Immobilon P. Blots were developed using an antibody against the N terminus of p34 C/EBP β (LAP) (26). The membranes were subsequently stained with Ponceau S to verify equal loading of GST proteins.

Synthetic Peptides and Recombinant TAZ2 Fragment—Purified human p300 TAZ2 polypeptide has been described (27). The C-terminal regulatory domain (CRD) peptide corresponds to aa 273–296 of rat C/EBP β and was purchased from Global Peptide Services; p53 peptide (aa 9–25 of human p53) was a gift from E. Appella.

p300/CBP Binding Assays—C/EBP β (WT, mLX1, mLX2, Δ AID) and p300/CBP (FLAG-tagged CBP_{1680–2441}, HA-tagged p300 WT, and d33) were expressed separately in 293T cells. Nuclear extracts were prepared, diluted in binding buffer (20 mM HEPES, pH 7.9, 100 mM NaCl, 0.1 mM EDTA, 0.1% Nonidet P-40), and mixed for 2 h at 4 °C prior to immunoprecipitation with anti-FLAG M2-agarose (Sigma) or mono HA.11 affinity matrix (Covance) overnight. The beads were washed six times with binding buffer and boiled in sample buffer, and the eluates analyzed for C/EBP β by Western blotting.

In Silico Studies—The C/EBP β primary structure was analyzed using several web-based servers available via the ExPASy site. Assessment of secondary structure and solvent accessibility for individual residues in the sequence was performed by the PHD method (28) included in the Predict-Protein package (29). The hydrophobic profile was obtained using ProtScale (30) run with the default window size (5 residues). Pre-Link (31) was used to predict flexible linker regions. Hydrophobic cluster analysis (32) uses a representation of protein sequence on an α -helical two-dimensional pattern to better visualize structural features and the environment of each amino acid in the protein sequence. Sets of adjacent hydrophobic residues in the pattern are termed hydrophobic clusters. The shapes of these clusters and their distribution along the sequence provide useful guidance for predictions of regular secondary structure elements and protein tertiary fold (reviewed in Ref. 33).

RESULTS

C/EBP β DNA Binding Is Auto-repressed by N-terminal Sequences and Becomes Activated by Oncogenic Ras Signaling—We recently reported that DNA binding of the major C/EBP β isoform, p34 LAP (aa 22–297), is suppressed and becomes stimulated by oncogenic Ras signaling (18). To further investigate regulation of C/EBP β DNA binding, we addressed the mechanism of auto-inhibition. C/EBP β was expressed in HEK293T

cells without or with H-Ras^{V12}, and nuclear extracts normalized for C/EBP β levels were analyzed by EMSA using a consensus C/EBP site probe. As shown in Fig. 1A, Ras induced a significant increase in C/EBP β DNA binding when compared with its activity without Ras. The shifted protein species in lane 2 of the Western blot corresponds to phospho-Ser-64 (21), which does not regulate DNA binding, but its presence confirms C/EBP β activation by Ras signaling. The binding activity of endogenous C/EBP β in primary mouse fibroblasts is also induced by H-Ras^{V12} (18), showing that stimulation of C/EBP β DNA binding is a physiological response to Ras.

A truncated protein containing only the C-terminal bZIP DNA-binding domain (DBD) displayed much higher basal activity that was not further stimulated by Ras (Fig. 1A, lanes 5 and 6). Thus, C/EBP β DNA binding in unstimulated cells is constrained by sequences located in the N-terminal region, and this auto-repression is overcome by Ras signaling. A construct containing the N-terminal transactivation domain (TAD; aa 22–104) fused to the DBD (aa 212–297), denoted 22–104/DBD, was also partially inhibited and derepressed by Ras (lanes 3 and 4). Thus, the TAD region itself has inhibitory effects on DNA binding. Transactivation assays using a C/EBP-driven reporter (2 \times C/EBP-Luc) showed that C/EBP β (LAP) possesses low basal transcriptional activity that is strongly increased (\sim 20-fold) by Ras^{V12} (Fig. 1B). 22–104/DBD displayed higher basal transactivation, and its Ras-induced activity was also increased relative to LAP, whereas DBD did not appreciably activate transcription because it lacks a TAD.

To provide additional evidence for intrinsic repression of C/EBP β , we analyzed DNA binding of purified, bacterially expressed proteins (Fig. 1C). C/EBP β (LAP) binding was undetectable, whereas 22–104/DBD binding was low but measurable, and DBD exhibited very high activity. These results are similar to those observed for the same proteins expressed in mammalian cells without Ras, strongly suggesting that low basal DNA binding is due to intrinsic inhibition by the N-terminal region.

To further define C/EBP β auto-inhibitory sequences, we analyzed a set of N-terminal deletion mutants (Fig. 2). 64–297, which lacks the N-terminal part of the TAD, was auto-repressed and was activated by Ras similarly to WT LAP (compare lanes 1–4). However, 102–297 (lacking the entire TAD) showed increased basal activity that was further stimulated by Ras. The enhanced basal activity observed upon removal of aa 64–102 indicates the presence of a repressive sequence within this interval. Deletion to aa 122 further derepressed basal activity, revealing another inhibitory sequence in the 102–122 interval.

Figs. 1A and 2 demonstrate that at least two elements are involved in auto-repression because sequences both N-terminal and C-terminal to aa 104 confer partial inhibition. Interestingly, the naturally occurring LIP isoform (153–297) displayed nearly undetectable binding activity and was refractory to Ras activation (Fig. 2, lanes 9 and 10). Thus, LIP apparently contains an auto-inhibitory element but lacks sequences required for activation by Ras. The differential regulation of LAP and LIP DNA binding was consistently observed and is currently under further investigation. Removal of sequences to aa 170 resulted

C/EBP β Auto-inhibition

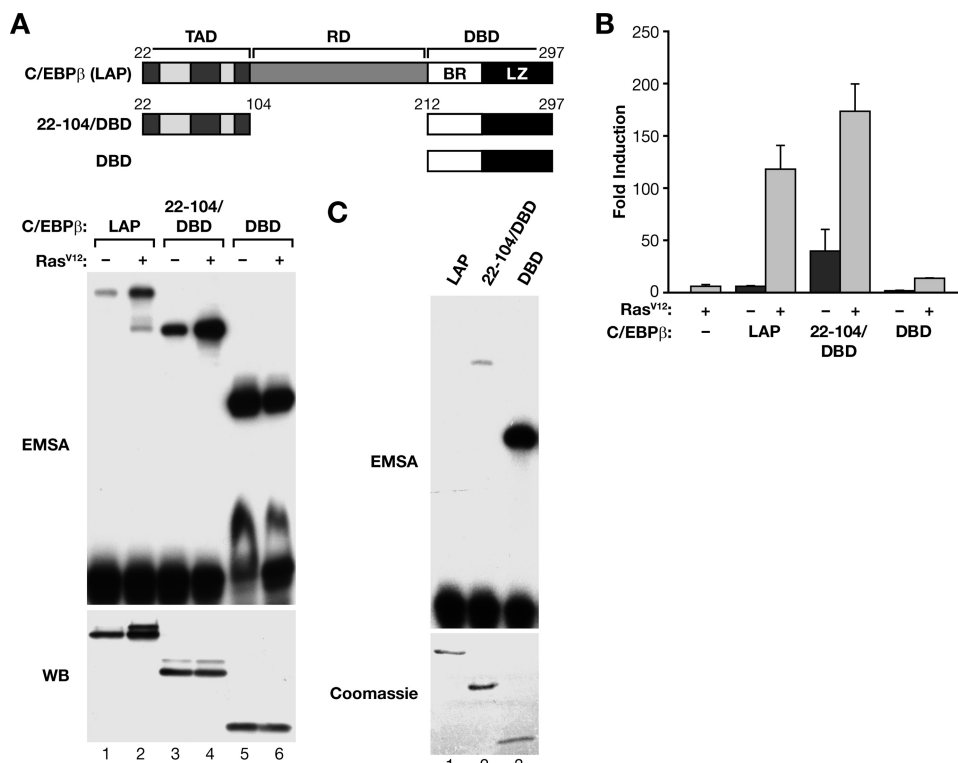


FIGURE 1. C/EBP β DNA binding activity is auto-inhibited by the N-terminal region and activated by oncogenic Ras signaling. *A*, diagram shows the rat C/EBP β p34 (LAP) isoform (aa 22–297) and deletion mutants; 22–104/DBD consists of the N-terminal transactivation domain fused to the DNA-binding domain. Proteins were expressed in 293T cells without or with oncogenic H-Ras^{V12}, and nuclear extracts were prepared after overnight serum starvation. After equalizing C/EBP β protein levels by Western blotting (WB, lower panel), the extracts were analyzed by EMSA using a radiolabeled consensus C/EBP probe. The upper band in lane 2 (LAP + Ras) corresponds to Ras-induced phosphorylation on Ser-64. *B*, C/EBP β proteins were analyzed in transactivation assays \pm Ras^{V12} using a C/EBP-driven reporter, 2 \times C/EBP-luc. Cells were harvested for luciferase assays after overnight serum starvation. Normalized activity of the reporter alone was set to one, and all other values are expressed as -fold activation relative to the reporter. Data are the average (\pm S.E.) of three independent experiments. *C*, the C/EBP β proteins described in panel *A* were expressed in *E. coli*, purified, and analyzed by EMSA. Protein levels were equalized by SDS-PAGE/Coomassie Brilliant Blue staining (lower panel).

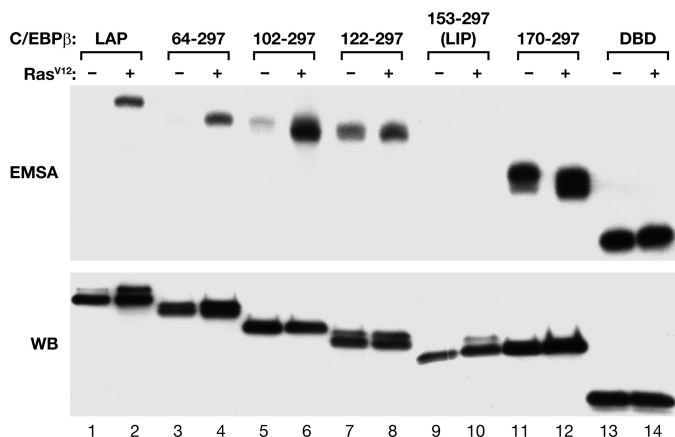


FIGURE 2. Deletion analysis of auto-inhibitory sequences. The indicated N-terminal C/EBP β deletions were expressed in 293T cells \pm Ras^{V12} and analyzed by EMSA. Numbers indicate residues included in each protein; LAP, aa 22–297. The lower portion of the gel containing the free probe was cropped to conserve space here and in subsequent figures. Bottom panel, C/EBP β Western blot (WB) of equalized cell extracts.

in a fully derepressed protein, similar to the DBD alone (lanes 11–14), thus identifying a third inhibitory region near the N terminus of LIP.

Insights from Sequence Analysis—

We next used several sequence analysis tools to search the C/EBP β sequence for regions of hydrophobicity and potential secondary structure as these properties are associated with elements involved in inter- or intraprotein interactions that could mediate auto-repression. The N-terminal region is mostly unstructured, with pockets of hydrophobicity and a few short segments of possible secondary structure, mainly α -helix (Fig. 3A). Some of the structured segments overlap with functional elements in the TAD. Prediction of linker regions and hydrophobic cluster analysis (Fig. 3B) suggested that the N-terminal region of LAP (aa 22–211) contains three folded subdomains denoted I (22–40), II (52–118), and III (143–171, corresponding to CR7 (17)). Subdomain I is populated by short hydrophobic helices, and II contains two helices (clusters IIa and IIb) and a short extended strand (cluster IIc) that overlaps with CR5. The shape of cluster III suggests that this region may comprise a combination of α -helix and extended strand structure. Subdomains I and II are connected by a short disordered linker, whereas II and III are separated by a hydrophobic but solvent-exposed Pro-rich loop. Subdomains I and II together encompass the TAD (22–104), which is composed of three conserved activation domain modules (14) that correspond to three hydrophobic helices within this region (I, IIa, and IIb). We also used the PHD method to predict the solvent accessibility of each amino acid (Fig. 3A). This analysis shows a preponderance of buried residues in regions associated with auto-repression (hydrophobic clusters IIb, IIc, and III). The N-terminal part with potential to fold into a globular structure (hereafter referred to as the N-terminal domain) is separated from the bZIP domain by a solvent-exposed region devoid of regular structure.

Clusters IIa and IIb coincide with the major activation domain module that binds to coactivators such as p300/CBP and TAF_{II}31 through an α -helical ϕ XX ϕ motif, LSDLF (Fig. 3A, boxed sequence) (14, 23, 34). Sequence inspection revealed a second ϕ XX ϕ -like motif in cluster III and a third within a region at the C/EBP β C terminus that mediates binding to c-Myb (35). The presence of buried ϕ XX ϕ motifs within two auto-inhibitory segments in the N-terminal region (Fig. 2) suggests that these sequences could mediate intramolecular interactions that stabilize the repressed conformation.

Clusters IIa and IIb coincide with the major activation domain module that binds to coactivators such as p300/CBP and TAF_{II}31 through an α -helical ϕ XX ϕ motif, LSDLF (Fig. 3A, boxed sequence) (14, 23, 34). Sequence inspection revealed a second ϕ XX ϕ -like motif in cluster III and a third within a region at the C/EBP β C terminus that mediates binding to c-Myb (35). The presence of buried ϕ XX ϕ motifs within two auto-inhibitory segments in the N-terminal region (Fig. 2) suggests that these sequences could mediate intramolecular interactions that stabilize the repressed conformation.

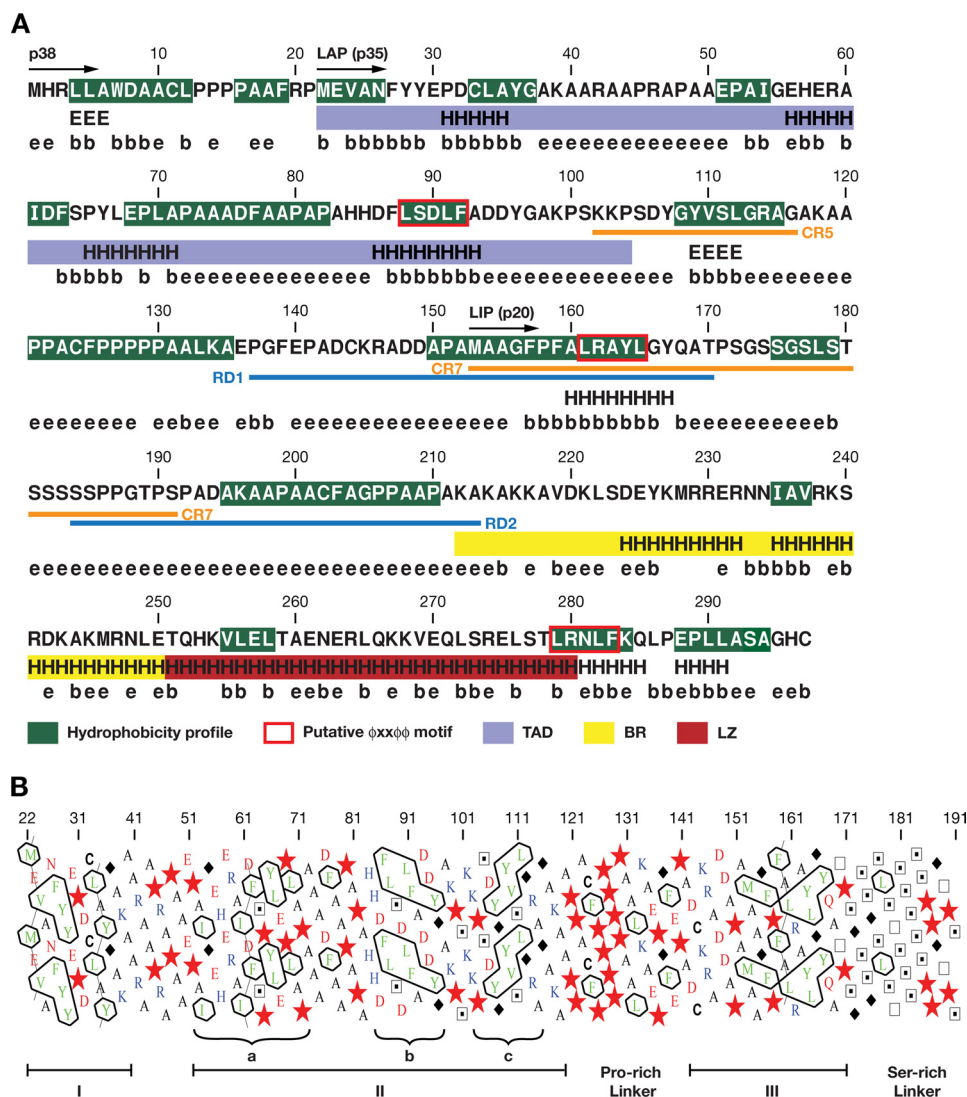


FIGURE 3. *In silico* analysis of the C/EBP β sequence. *A*, selected features of the rat C/EBP β amino acid sequence. Stretches of residues characterized by normalized hydrophobicity ≥ 0.5 (obtained with ProtScale (30)) are highlighted in green. Functional domains are indicated by colored bars: blue, TAD; yellow, BR; red, LZ. Predictions of secondary structure (*H*, helix; *E*, extended strand) and relative solvent accessibility (*e*, residues exposed with more than 36% of their surface; *b*, residues with less than 9% of surface exposed) as determined by the PHD method (28) are shown below the sequence. Boxes indicate $\phi X X \phi \phi$ -like motifs. Boundaries of the CR5/7 and RD1/2 auto-inhibitory domains are depicted. *B*, two-dimensional helical representation of the LAP N-terminal region (hydrophobic cluster analysis plot). The sequence is displayed on a cylinder representing an α -helix with 3.6 amino acids per turn. The cylinder is then cut parallel to its axis, unrolled, and duplicated to better visualize the environment of each amino acid. Hydrophobic residues are colored green; acidic residues are red; and basic residues are blue. Red star, prolines; diamond, glycines; open square, threonines; dotted square, serines. Hydrophobic clusters are encircled. Brackets below the hydrophobic cluster analysis plot indicate borders of the putative folded regions (designated I, II (a–c), and III) defined by the PreLink program (31).

Mutational Analysis of Auto-inhibitory Motifs—To assess the roles of the putative protein interaction elements in auto-repression, we generated site-directed mutations. Hydrophobic residues at positions 1, 4, and 5 of the $\phi X X \phi \phi$ motifs in the N-terminal region (LX1, aa 88–92; LX2, aa 161–165) were converted to Ala, and hydrophobic cluster IIc (aa 108–114), termed the AID, was deleted (Fig. 4A). mLX1 and mLX2 were constructed singly and in tandem, and Δ AID was created alone or with mLX1/2. Each of the single mutations caused a modest increase in basal DNA binding, with mLX2 having the largest effect, but they did not affect the Ras-induced binding (Fig. 4A). The double mutant mLX1/2 was slightly more active than

mLX2. Notably, the mLX1/2 Δ AID triple mutant was fully derepressed and was not further activated by Ras. Thus, the LX1, LX2, and AID motifs mediate auto-inhibition by the N-terminal region.

Transactivation assays showed that mutants containing mLX1 were very poor transcriptional activators, as expected because LX1 is a critical component of the TAD (Fig. 4B). The Ras-stimulated activity of mLX2 was nearly 3-fold higher than WT LAP, and Δ AID was at least 4-fold greater. Plotting the luciferase data on a different scale (*inset*) shows that these two mutations also enhanced basal activity. However, Ras-induced transcription was invariably much higher than the basal value, even for mutants whose unstimulated DNA binding activity was significantly derepressed. This suggests that Ras signaling also enhances the transcriptional potential of C/EBP β independently of DNA binding.

We next analyzed DNA binding of purified recombinant proteins containing a subset of the $\phi X X \phi \phi$ -like (LX) and AID mutations (Fig. 4C). mLX2 had a small enhancing effect, whereas mLX1/2 further increased DNA binding, and the activity of the triple mutant was even higher. Thus, the results of Fig. 4, A–C, show that C/EBP β is intrinsically repressed by three elements located in the N-terminal half of the protein.

$\phi X X \phi \phi$ α -helices often include charged residues that contribute to the specificity and stability of interactions with binding partners (36). LX1 is flanked by 3 Asp residues that form a negatively charged edge on the hydrophobic core (Figs. 3B and 4D). To investigate the function of these residues in auto-repression, we analyzed Asp \rightarrow Arg substitution mutants (D86R and D94R/D95R). Both mutants were auto-repressed; however, binding by the D86R mutant was only weakly activated by Ras, whereas D94R/D95R was completely resistant to activation (Fig. 4D). Transactivation by both of these mutants was also severely decreased (Fig. 4E). Thus, negatively charged residues flanking LX1 are not critical for auto-inhibition but play an important role in C/EBP β activation by Ras signaling, in agreement with previous data (37). The reduction in Ras-induced transcriptional activity by these mutants probably involves not only decreased DNA

C/EBP β Auto-inhibition

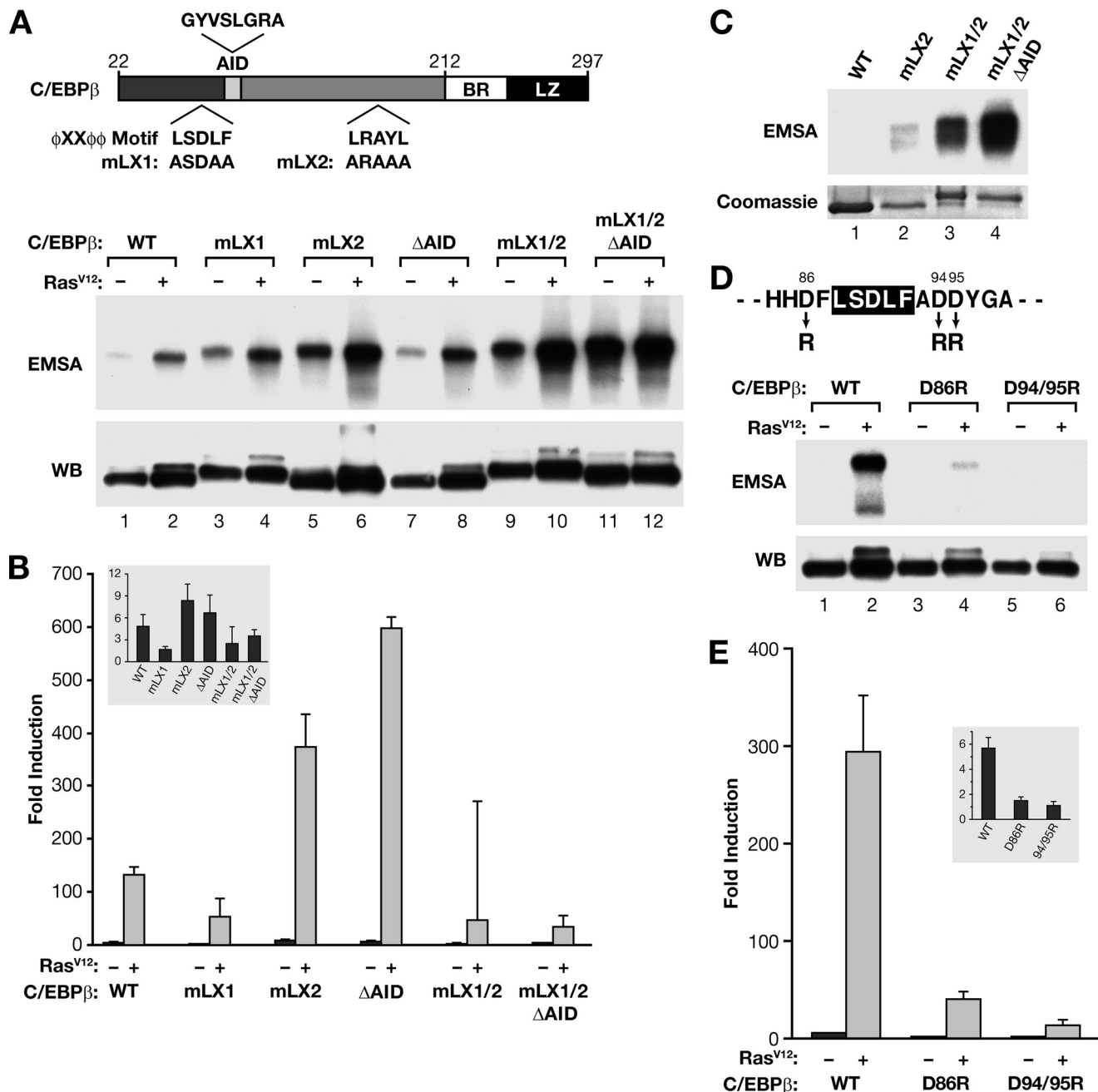


FIGURE 4. Mutational analysis of putative auto-inhibitory motifs. *A*, proposed regulatory elements and their mutant versions are depicted in the diagram. Two ϕ XX ϕ motifs and the AID were mutated by Ala substitution (mX1, mX2) or deletion (Δ AID), singly and in combination. Mutant proteins were expressed in 293T cells and tested by EMSA for basal and Ras-induced DNA binding. The mX1 mutation consistently reduces the mobility of C/EBP β in SDS-PAGE gels (see also *panel C* and Fig. 6C), most likely due to a conformational change. *WB*, Western blot. *B*, mutants were analyzed in transactivation assays using $2 \times$ C/EBP-Luc reporter. The *inset* shows the basal activities graphed on a different scale. *C*, the indicated proteins were expressed in *E. coli*, purified, and tested for DNA binding by EMSA. *Bottom*, protein levels used for EMSA. *D* and *E*, effects of mutating acidic residues flanking LX1. Mutants depicted in the diagram were assayed for DNA binding (*panel D*) and transactivation (*panel E*) in 293T cells. Results of three independent assays were averaged (\pm S.E.).

binding but also impaired interactions with coactivators (*e.g.* in the p300 TAZ2-p53 complex, p53 Glu-17, which is equivalent to C/EBP β Asp-86, forms a salt bridge interaction with TAZ2 Arg-1731 (38)).

Identification of Sequences in the bZIP Region Mediating Auto-inhibition—To identify elements in the DBD that participate in auto-inhibition, we generated a nested set of deletions that remove sequences from the C terminus and the end of the LZ (Fig. 5A). Deletion of aa 286–297 (STOP6) had little effect

on DNA binding. Resection to aa 279 (STOP5) led to reproducibly higher basal activity, implicating sequences between aa 279 and 286 in auto-repression. A protein ending at residue 272 (STOP4) displayed very low basal and Ras-induced binding activity, and further deletion completely eliminated DNA binding (data not shown). The latter results are probably due to disruption of LZ function and loss of dimerization. The CRD identified by these deletions also mediates cooperative interactions with c-Myb (35). We noted that it contains a ϕ XX ϕ

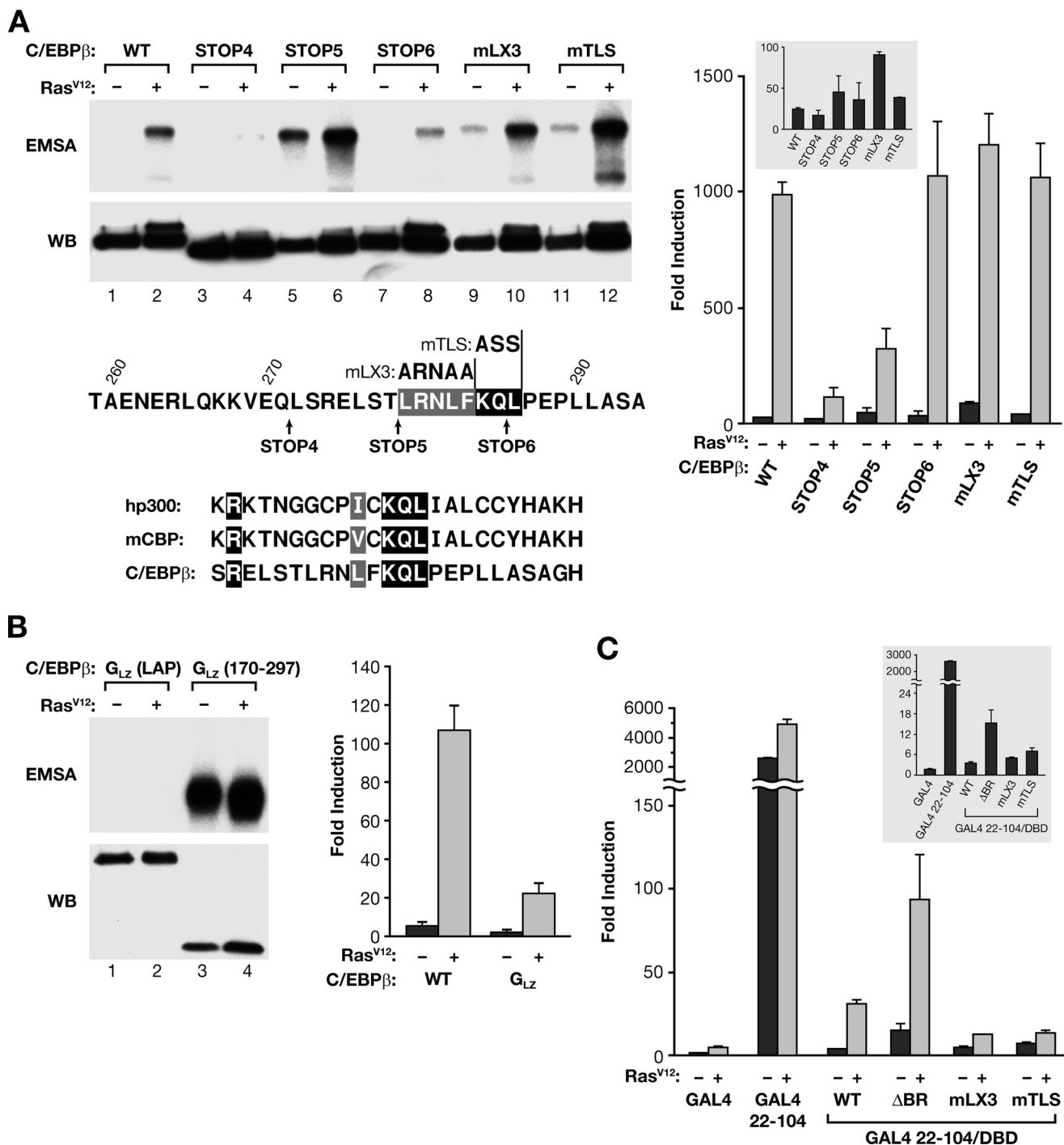


FIGURE 5. Identification of bZIP sequences mediating auto-inhibition. *A*, effects of mutations in putative C-terminal regulatory elements. The diagram shows the sequence of the C-terminal region indicating LX3 and the TLS and mutations in these elements and an alignment of the C/EBP β C terminus and the TAZ2 domains of human p300 and mouse CBP. STOP mutants contain termination codons at the repeated Leu residues, creating nested C-terminal deletions. DNA binding (*left*) and transactivation assays (*right*) were performed. *WB*, Western blot. The *inset* shows basal activity on a different scale. *B*, effect of a heterologous LZ on C/EBP β activation. C/EBP β -G_{LZ} is a chimeric LAP protein containing the GCN4 leucine zipper; G_{LZ}(170–297) is a truncated version. *Left*, DNA binding; *right*, transactivation assays of C/EBP β and C/EBP β -G_{LZ}. *C*, mutations in the bZIP domain were introduced into 22–104/DBD fused at its N terminus to GAL4 DBD. Constructs were co-transfected \pm Ras^{V12} with a GAL4-dependent reporter, G₅E1b-luc. GAL4-(22–104) contains the C/EBP β TAD alone fused to GAL4. Data are the average (\pm S.E.) of three independent experiments.

motif (LX3) as well as an amino acid triplet, KQL, which is also present in the TF-binding site of p300/CBP TAZ2. We named this element “TAZ-like sequence” or TLS (Fig. 5A, *diagram*). The region encompassing LX3 and TLS shows similar hydrophobicity to the TAZ2 helix that mediates p300/CBP binding to the p53 TAD and other TFs (Ref. 39 and references therein),

including to C/EBP β via LX1. Significantly, Gln of the p300 KQL motif forms a buried hydrogen bond with aspartic acid from the p53 TAD “signature helix” (FSDLW) (38). Therefore, by analogy to the p53-TAZ2 interaction, we hypothesized that the C/EBP β C terminus may participate in binding to N-terminal inhibitory sequences such as LX1 (LSDLF).

C/EBP β Auto-inhibition

Mutation of LX3 and TLS caused a modest but reproducible increase in basal DNA binding and enhanced activation by Ras (Fig. 5A, lanes 9–12), indicating a role in auto-inhibition. The STOP5, mLX3, and mTLS mutants showed similar derepression when introduced into 22–104/DBD (data not shown). We further examined the role of the LZ region by analyzing a chimeric protein containing the GCN4 LZ (C/EBP β -G_{LZ}) (14). C/EBP β -G_{LZ} DNA binding was completely repressed and was refractory to Ras activation (Fig. 5B, lanes 1 and 2); transactivation was similarly impaired. The reduced activity of C/EBP β -G_{LZ} is not due to an inability of the chimeric DBD to bind DNA because an N-terminally truncated version of this protein (170–297) showed robust DNA binding (lanes 3 and 4). We conclude that the GCN4 LZ contains sequences capable of making inhibitory interactions with the C/EBP β N-terminal region but lacks elements required for activation, such as the RSK phosphorylation site (Ser-273) recently identified in the C/EBP β LZ (18).

Previous studies showed that the C/EBP β TAD is inhibited by the bZIP region and by central regulatory domains (14, 16). To further investigate the basis for this inhibition and to identify repressive sequences in the bZIP domain, we fused WT and mutant 22–104/DBD constructs to the GAL4 DBD and analyzed the ability of these chimeras to activate a GAL4 reporter gene (Fig. 5C). GAL4-(22–104/DBD) activity was auto-repressed and was stimulated nearly 30-fold by Ras, much like native C/EBP β (LAP), whereas GAL4-(22–104) displayed constitutively high activity. GAL4-LAP was also repressed and could be activated by Ras (data not shown). Thus, the bZIP region inhibits the TAD, and this repression can be reversed by Ras signaling. Deletion of the basic region in GAL4-(22–104/DBD) caused a 5-fold increase in basal transactivation and a 3-fold increase in Ras-induced activity when compared with WT. Therefore, the BR plays a critical role in auto-inhibitory interactions between the TAD and DBD. Mutating LX3 or TLS also slightly increased basal activity. Interestingly, Ras-induced transcription by these mutants was decreased relative to GAL4-(22–104/DBD), in contrast to the increased DNA binding and unaltered transactivation observed for the same mutations in native C/EBP β (Fig. 5A). These findings suggest that the auto-inhibitory LX3 and TLS elements can also play a positive role in transcription depending on the promoter context.

Physical Interactions Involving the N-terminal Auto-inhibitory Domain and the DBD—We next used GST pulldown assays to assess physical interactions between N-terminal sequences and the DBD (bZIP region). For these experiments, we analyzed binding of GST·DBD to two N-terminal C/EBP β polypeptides, 22–104 and 22–192. Both fragments bound to GST·DBD but not to GST alone (Fig. 6A). The addition of various divalent cations to the pulldown reaction showed that 22–104 binding to GST·DBD was relatively unaffected by the addition of Ca²⁺, Mg²⁺, or Zn²⁺, whereas 22–192 binding was strongly enhanced by Zn²⁺ (Fig. 6B). It is possible that Zn²⁺ ions enhance auto-inhibitory interactions by cross-linking residues from 104–192 to the bZIP region. However, the molecular/structural basis for the Zn²⁺ effect and the divalent cation specificity remains to be determined.

To determine whether the auto-inhibitory motifs are required for binding of the N-terminal sequences to the DBD, we analyzed several mutants. Introduction of mLX1 into 22–104 prevented its association with GST·DBD, and the mLX1/mLX2/ Δ AID 22–192 mutant also showed greatly reduced binding (Fig. 6C). Thus, sequences required for C/EBP β auto-repression mediate physical association with the DBD region. We next analyzed mutant versions of GST·DBD to determine which sequences in the bZIP domain are required for interaction with the N terminus. Deletion of the basic region strongly impaired binding to 22–192 (Fig. 6D), whereas STOP5, mLX3, and mTLS also reduced the association, albeit less severely. Because RSK-mediated phosphorylation of Ser-273 in the LZ is required for Ras-induced DNA binding (18), we examined S273A and S273D mutations. The S273A mutation had little effect on binding to 22–192 (lane 5), whereas the phosphomimetic S273D substitution decreased this interaction (lane 6). These findings support the idea that Ser-273 phosphorylation disrupts intramolecular interactions with the N-terminal region that mediate auto-inhibition.

Our results suggest that C/EBP β auto-repression involves contacts between the CRD region and the TAD LX1 motif, which also binds to CBP/p300 via TAZ2. If this model is correct, auto-inhibition should be disrupted by competitive binding of peptides that interact with LX1. To test this possibility, we incubated purified TAZ2 domain of p300 (27) with bacterially expressed 22–104/DBD and analyzed DNA binding. Binding was strongly enhanced by TAZ2, whereas a control p53 peptide had no effect (Fig. 7A, top panel). Derepression was also induced by a synthetic CRD peptide from C/EBP β that encompasses LX3 and TLS. In contrast, DBD DNA binding was not stimulated by any of the peptides, ruling out nonspecific effects (Fig. 7A, bottom panel). The TAZ2 and CRD peptides also stimulated the binding of repressed C/EBP β (LAP) expressed in 293T cells, whereas the p53 peptide had no effect (Fig. 7B). Again, binding of the constitutively active DBD protein was unaffected by the competitor peptides. These data further support the idea that LX1 interacts with sequences at the C terminus to inhibit C/EBP β activity.

C/EBP β Binding to p300/CBP Coactivators Requires the N-terminal Auto-inhibitory Elements—C/EBP β was reported to interact with p300/CBP coactivators via LX1 (34, 40, 41). Subsequently, the region C-terminal to the TAD was shown to also have a role in CBP binding (23). Because AID and LX2 are within this region and exhibit features of protein interaction domains, we hypothesized that they might participate in association with p300/CBP. Therefore, we used co-immunoprecipitation to assess binding of WT and mutant C/EBP β proteins to a C-terminal segment of CBP encompassing TAZ2 (CBP_{1680–2441}) (23). WT C/EBP β was expressed without or with Ras^{V12} in 293T cells, and extracts were incubated with a lysate from cells expressing FLAG-CBP_{1680–2441}. Following immunoprecipitation with FLAG antibody, C/EBP β in the bound fraction was analyzed by Western blotting (Fig. 8A). Efficient binding to CBP_{1680–2441} occurred only when C/EBP β was expressed in the presence of Ras^{V12} (compare lanes 1 and 2), demonstrating that

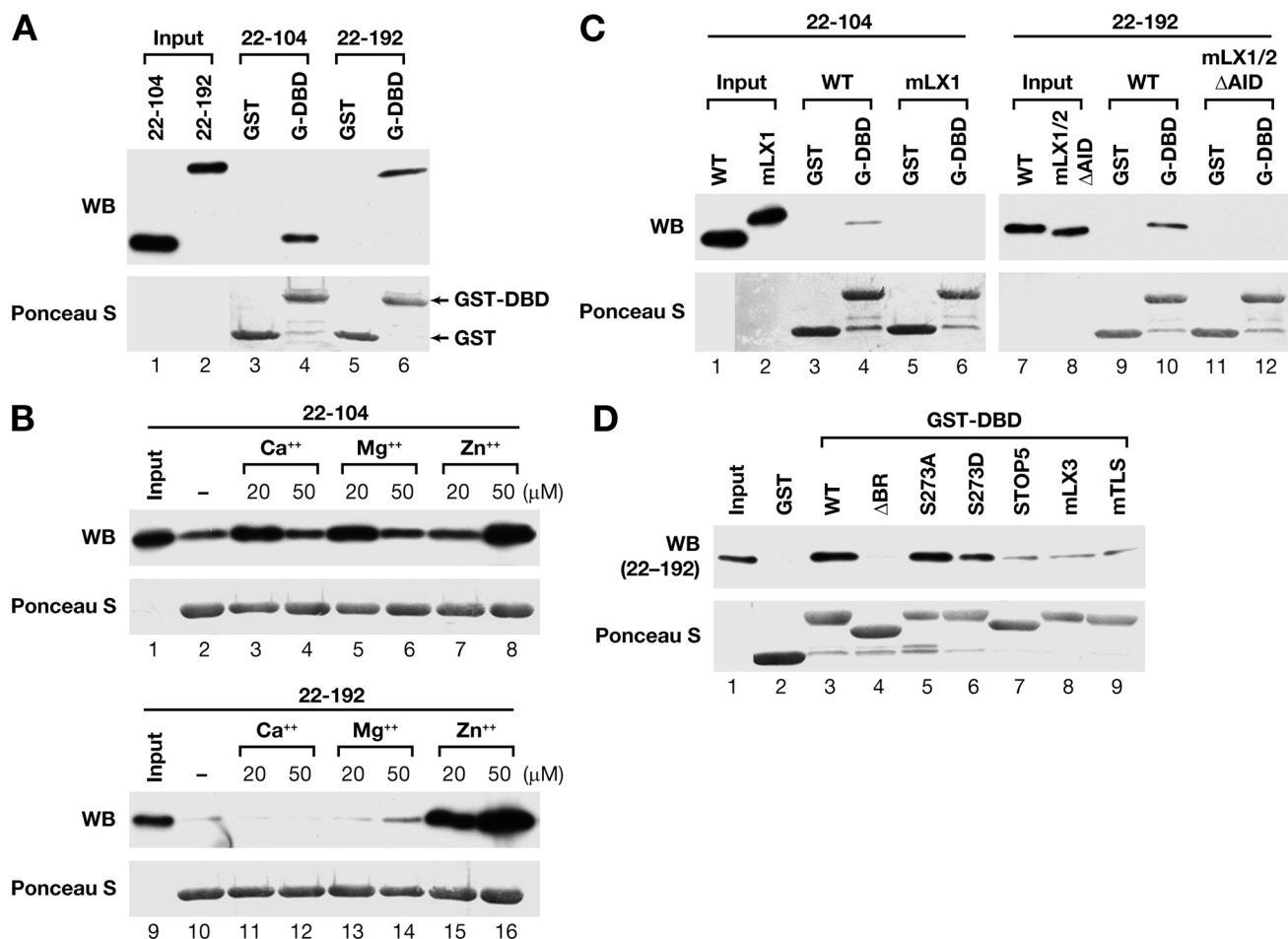


FIGURE 6. *C/EBPβ* auto-inhibitory sequences physically interact with the bZIP domain. *A*, *C/EBPβ* 22-104 or 22-192 fragments were expressed in *E. coli*, purified, and analyzed for binding to GST-DBD (aa 212–297) in pull-down assays. GST alone was used as a control. Bound proteins were eluted and analyzed by Western blotting (WB) using an antibody against the *C/EBPβ* (LAP) N terminus (upper panel). 1% of input is shown in lanes 1 and 2. The membrane was stained with Ponceau S to visualize GST proteins (lower panel). *B*, effects of various divalent cations on binding of 22-104 or 22-192 to the DBD. Proteins were analyzed in GST-DBD pull-down assays without (lanes 2 and 10) or with the indicated concentrations of Ca²⁺, Mg²⁺, or Zn²⁺. *C*, mutation of auto-inhibitory elements disrupts binding to the DBD. The indicated mutations were introduced into the 22-104 and 22-192 polypeptides, and the recombinant proteins were analyzed for binding to GST-DBD in the presence of 20 μM Zn²⁺. *D*, effects of mutations in the bZIP domain on binding to the N-terminal region. DBD mutants were fused to GST, and the expressed proteins were absorbed to glutathione beads, equalized for GST levels, and analyzed for binding to 22-192 in the presence of 20 μM Zn²⁺.

activated *C/EBPβ* is uniquely capable of making this association. Notably, each of the auto-inhibitory domain mutants (mLX1, mLX2, ΔAID) expressed with Ras displayed greatly reduced CBP binding (lanes 3–5). Identical results were obtained using HA-tagged p300; *i.e.* interaction with *C/EBPβ* required activation by Ras, and the auto-inhibitory domain mutants failed to bind p300. Furthermore, a p300 mutant lacking critical sequences in the TAZ2 domain (p300 d33) (24) displayed reduced binding to WT *C/EBPβ*, confirming that association with p300 involves TAZ2.

These findings were further corroborated in transactivation assays (Fig. 8*B*). Co-expression of p300 stimulated *C/EBPβ*-driven transcription of the 2× *C/EBP*-luc reporter by ~2-fold ($p = 0.02$). This augmentation occurred only in the presence of Ras signaling and did not affect basal *C/EBPβ* activity. However, none of the N-terminal auto-inhibitory domain mutants showed significant stimulation by p300 despite increased Ras-induced transcriptional activity of mLX2 and ΔAID due to their impaired auto-inhibition (see also Fig. 4*B*). Collectively, the data of Fig. 8, *A* and *B*, strongly suggest that activated *C/EBPβ*

binds to p300/CBP via the LX1, LX2, and AID elements, which also play critical roles in auto-repression.

DISCUSSION

The involvement of *C/EBPβ* in cellular responses to oncogenic Ras or Raf (9–12) suggested that its activity may be regulated by Ras signaling. Previous work demonstrated that the transcriptional potential of *C/EBPβ* is stimulated by activated Ras or other kinase oncogenes (9, 16, 42). In the present study, we have extended these findings and show that *C/EBPβ* DNA binding activity is auto-repressed and becomes activated in cells expressing oncogenic Ras^{V12}. Earlier studies identified auto-inhibitory regions CR5/7 (16) and RD1/2 (14) and roughly mapped their boundaries based on sequence conservation or deletion analysis. Here we show that three distinct N-terminal sequences that are predicted to form secondary structures inhibit *C/EBPβ* DNA binding. These include AID, which is located within CR5, and two LX motifs. In addition, the LX3 and TLS motifs in the CRD region contribute to auto-inhibi-

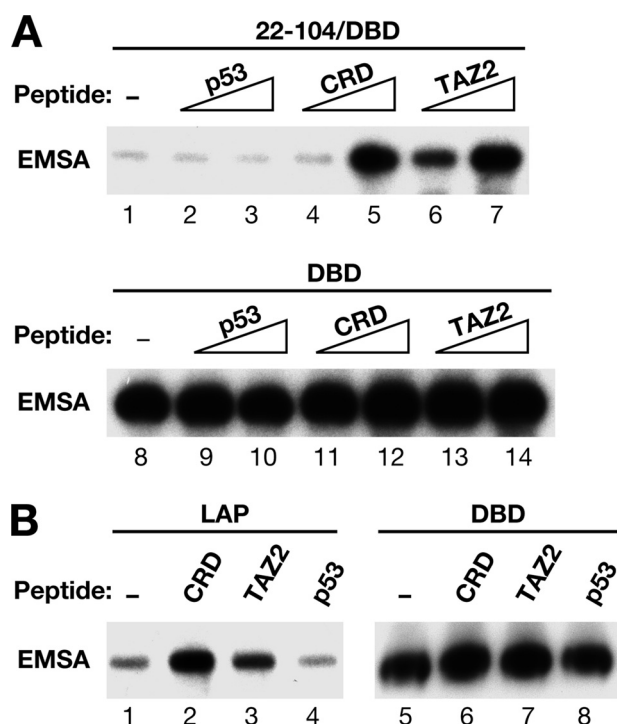
C/EBP β Auto-inhibition

FIGURE 7. C/EBP β DNA binding is activated by the presence of p300 TAZ2 or a C/EBP β C-terminal peptide. *A*, bacterially expressed 22–104/DBD and DBD were incubated with 0, 0.1, or 1 μ g of the competitor protein/peptide, and DNA binding was assessed by EMSA. CRD is a synthetic peptide encompassing C/EBP β aa 273–296; TAZ2 is a purified protein corresponding to the p300 TAZ2 domain. A peptide containing aa 9–25 of human p53 was used as a negative control. *B*, a similar peptide competition experiment was performed using nuclear extracts from 293T cells expressing C/EBP β (LAP) (lanes 1–4) or DBD (lanes 5–8) in the absence of Ras^{V12}.

tion. Thus, our study now provides a more detailed model of C/EBP β auto-inhibition.

We propose that the repressed conformation of C/EBP β involves a hydrophobic core formed by association of the N-terminal inhibitory elements and the CRD, as depicted in Fig. 8C. The TAD alone also confers partial repression (Fig. 1), and LIP, which contains only LX2/cluster III, is strongly auto-inhibited (Fig. 2).⁴ These results suggest that an inhibited structure can be formed by subsets of the N-terminal repressive elements. However, optimal repression of DNA binding and transactivation requires all three sequences.

The basic region appears to be a critical target of inhibition by the N-terminal region. We hypothesize that intramolecular interactions between the N-terminal domain and CRD induce a stable fold that generates a binding site for the BR, which is unstructured in the absence of DNA (43, 44), and this interaction prevents the BR from binding to DNA. Association of the BR with the N-terminal domain may involve electrostatic attractions between basic residues and negatively charged amino acids in the TAD region and/or hydrophobic interactions involving aliphatic portions of specific basic amino acid side chains. This mode of interactions involving both hydrophobic and electrostatic components mediates binding of Lys/Arg clusters from bipartite nuclear localization sequences to importin- α /Kap α (45). X-ray crystallography of the C/EBP α

bZIP domain bound to DNA showed that a single conserved Arg residue in the BR plays a critical role in the DNA-protein interface, and mutating this amino acid abrogates DNA binding (46). Thus, sequestration of the analogous residue (Arg-230) in auto-repressed C/EBP β may be sufficient to inhibit its binding activity. Further structural and mutagenesis studies are required to elucidate the detailed intramolecular interactions that repress C/EBP β DNA binding.

X-ray crystallography of the C/EBP β DBD in complex with c-Myb, which cooperates with C/EBP β to activate myeloid-specific genes such as *mim-1* (47–49), showed that the CRD region adjacent to the canonical LZ domain interacts with a subdomain of c-Myb to form a four-helix bundle (35). However, in the absence of c-Myb, the CRD segment is disordered. Thus, CRD is available to participate in formation of the stable hydrophobic core of auto-inhibited C/EBP β , as depicted in Fig. 8C. It is interesting to consider that interaction of CRD with cooperating TFs such as c-Myb on specific promoters could stimulate C/EBP β DNA binding and transactivation by disrupting the hydrophobic core and stabilizing the activated form of the protein. This model offers an appealing mechanism to explain the functional cooperativity between these two TFs (47–49).

Although mutating LX3 and TLS was expected to increase the transcriptional activity of C/EBP β by disrupting auto-repression, GAL4-(22–104/DBD) chimeras bearing these mutations instead showed decreased transactivation potential (Fig. 5C). Therefore, the CRD may positively regulate transcription from certain promoters. It is possible that CRD mediates interaction with coactivators or cooperating TFs such as c-Myb in specific promoter contexts. In support of this idea, the C/EBP β LZ/C-terminal region is known to play a key role in lipopolysaccharide-induced activation of pro-inflammatory cytokine genes (50, 51), and a sequence at the C terminus specifies the ability of C/EBP α , but not C/EBP β , to activate the CYP2D5 cytochrome P450 gene in hepatic cells (52). Thus, the CRD regions of C/EBP family members, all of which harbor ϕ XX ϕ motifs, may contribute to the distinct regulatory functions of each protein.

The inability of LIP to bind DNA, even in response to Ras, was unexpected but was observed in multiple cell lines.⁴ The resistance to Ras activation is highly specific to LIP because deletions ending before and after the LIP start site display Ras-induced or constitutive DNA binding (Fig. 2). Interestingly, a similar pattern of activity was seen for a panel of C/EBP β deletion mutants analyzed for lipopolysaccharide-induced activation of the *MCP-1* gene (53). These results suggest that LIP DNA binding is indeed regulated differently from LAP and may contribute to its distinct biological functions. The mechanistic basis for differential regulation of LIP and LAP is presently unclear and is under further investigation. Although LIP is a transcriptional inhibitor, it can also function as an activator in conjunction with other TFs on specific target promoters (54). The fact that LIP contains LX2 raises the possibility that this C/EBP β isoform provides a partial p300/CBP-binding site and thus could function cooperatively with other TFs to recruit coactivators to certain promoters.

⁴ S. Lee and P. F. Johnson, unpublished data.

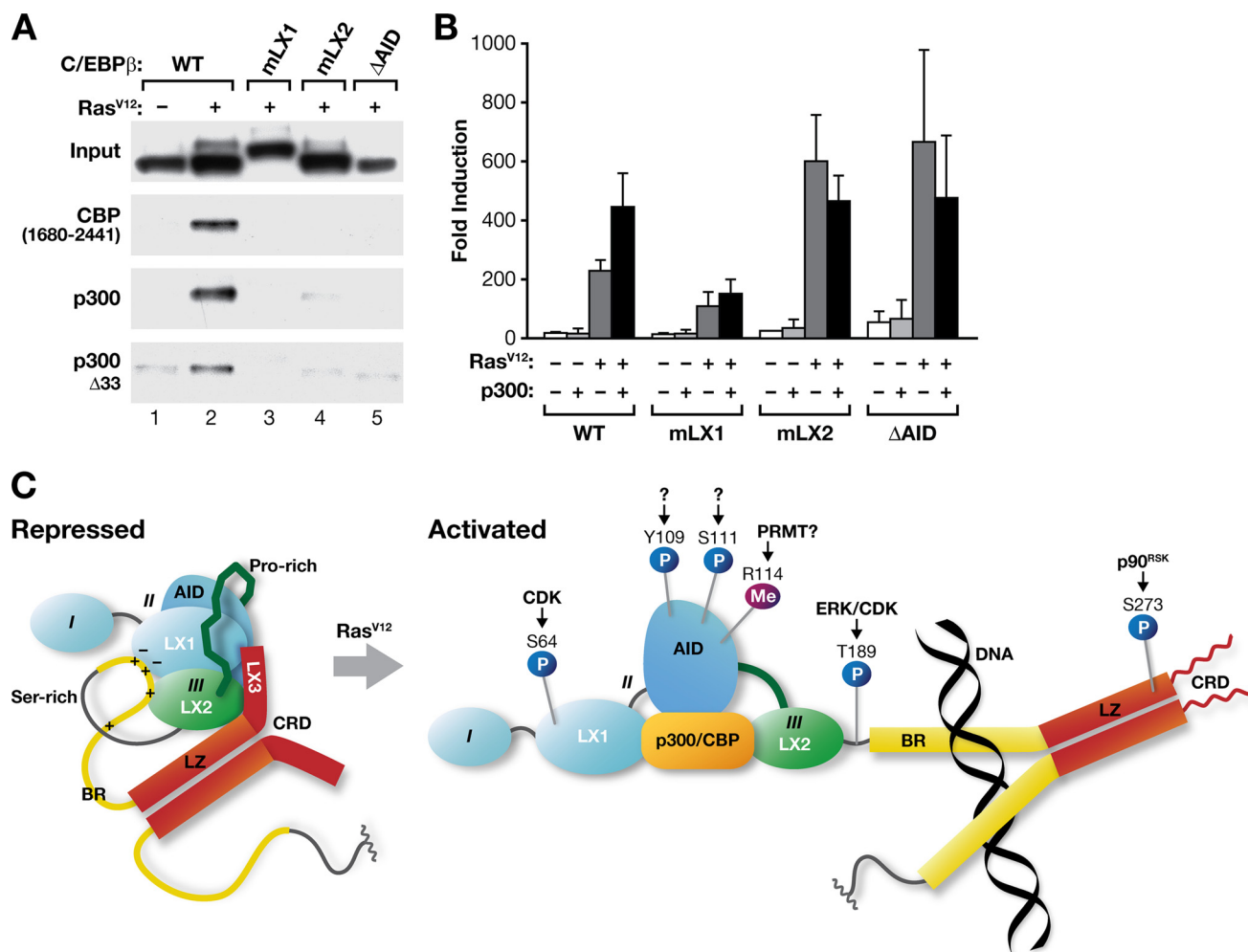


FIGURE 8. Binding of activated C/EBP β to p300/CBP requires the N-terminal auto-inhibitory elements. *A*, WT and mutant C/EBP β proteins were expressed in 293T cells without or with Ras^{V12}, and nuclear extracts were prepared. Normalized extracts (*top row*) were mixed with cell lysates containing FLAG-CBP_{1680–2441}, HA-p300, or p300 TAZ2 mutant d33. After immunoprecipitation using the appropriate tag antibodies, C/EBP β was analyzed by Western blotting. *B*, p300 stimulates C/EBP β transcriptional activity in the presence of Ras signaling. 293T cells were transfected with 2 \times C/EBP-luc and the indicated vectors, and luciferase activity was determined. Results of three independent assays were averaged (\pm S.E.). *C*, model for C/EBP β auto-inhibition and Ras-induced activation. Hydrophobic subdomains I, II, and III are shown together with Pro-rich and Ser-rich connecting loops. A stable hydrophobic core composed of LX1, AID, LX2, and the C-terminal CRD region encompassing LX3 and TLS is formed in the repressed state. We envision that interaction of the BR with the negatively charged surface of the folded N-terminal domain inhibits DNA binding. The TAD is also sequestered, repressing transactivation. Ras signaling induces phosphorylation on Ser-273 (p90^{RSK}) as well as phosphorylation on Tyr-109/Ser-111 (unknown kinases) and monomethylation of Arg-114. Ser-64 (Cdk) and Thr-189 (ERK, Cdk) are also inducibly phosphorylated but do not regulate DNA binding. We propose that phospho-Ser-273, Tyr-109, and Ser-111 activate C/EBP β in part through repulsion of negatively charged amino acids in the N-terminal domain. Upon activation, C/EBP β binds to p300/CBP via LX1, AID, and LX2.

Activation of C/EBP β DNA binding by oncogenic Ras integrates the effects of several post-translational modifications, as depicted in Fig. 8C. Ras-induced derepression requires signaling through the Raf-MEK-ERK cascade and involves RSK-mediated phosphorylation on Ser-273 in the LZ (18). Ras^{V12} also stimulates phosphorylation on Tyr-109 and Ser-111 and monomethylation of Arg-114, which are located in the AID region and are necessary for efficient Ras-induced activation of C/EBP β DNA binding (18). Thus, inducible phosphorylation within or near the AID and CRD domains stimulates binding activity. Moreover, three negatively charged amino acids flanking LX1 (Asp-86, -94, and -95) are critical for induction of DNA binding (Fig. 4D). It is possible that these acidic residues act via a charge repulsion mechanism involving phospho-Tyr-109, Ser-111, and Ser-273 and perhaps other modifications. Upon phosphorylation, electrostatic repulsion overcomes intramo-

lecular interactions that maintain the folded core of the repressed protein (Fig. 8C). In support of this model, the S273D phosphomimetic mutation decreased binding between the DBD and the N-terminal region in pulldown assays. Future studies should reveal whether other modifications (*e.g.* affecting LX1 and LX2) are also involved in C/EBP β derepression.

The LX1 motif is both an auto-inhibitory element and a signature ϕ XX ϕ helix with similarity to TAD motifs in other TFs (*e.g.* p53) that mediate binding to p300/CBP and TAF_{II}31 (34, 40). We propose that LX1 is sequestered within the hydrophobic core of repressed C/EBP β , rendering it inaccessible to coactivators and ensuring that transactivation as well as DNA binding is suppressed (Fig. 8C). This view is supported by GAL4 fusion experiments showing that the transcriptional activity of C/EBP β is constrained by CR5/AID and the DBD region, and this can be reversed by Ras signaling (14, 16) (Fig. 5C).

C/EBP β Auto-inhibition

The fact that CR5/AID and LX2 are essential for p300/CBP binding shows that the interaction with these coactivators is more complex than previously envisioned and probably involves multiple contacts in both proteins. Indeed, a previous study showed that sequences in the C/EBP β TAD cluster IIa region (aka "Box A" (55)) are also involved in CBP binding (23). The CR5/AID and LX2 regions have not been associated with activating functions, and it is possible that the systems previously used to assess C/EBP β transcriptional activity, including the reporter assays employed in our study, do not require p300/CBP as a coactivator. The critical role of the LX1 motif in transient reporter assays suggests that another coactivator or adapter protein, possibly TAF_{II}31, that interacts primarily via LX1 is essential for transcription in this setting. It is conceivable that p300/CBP recruitment is more relevant for activation of endogenous genes in a native chromatin environment, where basal transcription is stringently suppressed and histone acetylation is critical for gene induction. Thus, it will be of interest to determine whether AID and LX2 indeed contribute to transcription of specific chromatin-embedded target genes.

Acknowledgments—We thank Carlton Briggs for purification of recombinant proteins, Nancy Martin for expert technical assistance, William Sellers for p300 plasmids, Jean-Rene Cardinaux for CBP vectors, Allan Kane and Jiro Wada for preparation of figures, and Cindy Zahnnow for critical reading of the manuscript.

REFERENCES

- Whitmarsh, A. J., and Davis, R. J. (2000) *Cell Mol. Life Sci.* **57**, 1172–1183
- Chrivia, J. C., Kwok, R. P., Lamb, N., Hagiwara, M., Montminy, M. R., and Goodman, R. H. (1993) *Nature* **365**, 855–859
- Weigel, N. L., and Moore, N. L. (2007) *Mol. Endocrinol.* **21**, 2311–2319
- Graves, B. J., Cowley, D. O., Goetz, T. L., Petersen, J. M., Jonsen, M. D., and Gillespie, M. E. (1998) *Cold Spring Harb. Symp. Quant. Biol.* **63**, 621–629
- Jonsen, M. D., Petersen, J. M., Xu, Q. P., and Graves, B. J. (1996) *Mol. Cell Biol.* **16**, 2065–2073
- Eferl, R., and Wagner, E. F. (2003) *Nat. Rev. Cancer* **3**, 859–868
- Ramji, D. P., and Foka, P. (2002) *Biochem. J.* **365**, 561–575
- Sebastian, T., and Johnson, P. F. (2006) *Cell Cycle* **5**, 953–957
- Zhu, S., Yoon, K., Sterneck, E., Johnson, P. F., and Smart, R. C. (2002) *Proc. Natl. Acad. Sci. U.S.A.* **99**, 207–212
- Wessells, J., Yakar, S., and Johnson, P. F. (2004) *Mol. Cell Biol.* **24**, 3238–3250
- Sebastian, T., Malik, R., Thomas, S., Sage, J., and Johnson, P. F. (2005) *EMBO J.* **24**, 3301–3312
- Kuilman, T., Michaloglou, C., Vredeveld, L. C., Douma, S., van Doorn, R., Desmet, C. J., Aarden, L. A., Mooi, W. J., and Peeper, D. S. (2008) *Cell* **133**, 1019–1031
- Collado, M., Blasco, M. A., and Serrano, M. (2007) *Cell* **130**, 223–233
- Williams, S. C., Baer, M., Dillner, A. J., and Johnson, P. F. (1995) *EMBO J.* **14**, 3170–3183
- Kim, J., Cantwell, C. A., Johnson, P. F., Pfarr, C. M., and Williams, S. C. (2002) *J. Biol. Chem.* **277**, 38037–38044
- Kowenz-Leutz, E., Twamley, G., Ansieau, S., and Leutz, A. (1994) *Genes Dev.* **8**, 2781–2791
- Katz, S., Kowenz-Leutz, E., Müller, C., Meese, K., Ness, S. A., and Leutz, A. (1993) *EMBO J.* **12**, 1321–1332
- Lee, S., Shuman, J. D., Guszczynski, T., Sakchaisri, K., Sebastian, T., Copeland, T. D., Miller, M., Cohen, M. S., Taunton, J., Smart, R. C., Xiao, Z., Yu, L. R., Veenstra, T. D., and Johnson, P. F. (2010) *Mol. Cell Biol.* **30**, 2621–2635
- Darimont, B. D., Wagner, R. L., Apreletti, J. W., Stallcup, M. R., Kushner, P. J., Baxter, J. D., Fletterick, R. J., and Yamamoto, K. R. (1998) *Genes Dev.* **12**, 3343–3356
- Yamamoto, K. R., Darimont, B. D., Wagner, R. L., and Iñiguez-Lluhi, J. A. (1998) *Cold Spring Harb. Symp. Quant. Biol.* **63**, 587–598
- Shuman, J. D., Sebastian, T., Kaldis, P., Copeland, T. D., Zhu, S., Smart, R. C., and Johnson, P. F. (2004) *Mol. Cell Biol.* **24**, 7380–7391
- McKnight, S. L., and Kingsbury, R. (1982) *Science* **217**, 316–324
- Kovács, K. A., Steinmann, M., Magistretti, P. J., Halfon, O., and Cardinaux, J. R. (2003) *J. Biol. Chem.* **278**, 36959–36965
- Eckner, R., Ewen, M. E., Newsome, D., Gerdes, M., DeCaprio, J. A., Lawrence, J. B., and Livingston, D. M. (1994) *Genes Dev.* **8**, 869–884
- Kapust, R. B., Tözsér, J., Fox, J. D., Anderson, D. E., Cherry, S., Copeland, T. D., and Waugh, D. S. (2001) *Protein Eng.* **14**, 993–1000
- Williams, S. C., Cantwell, C. A., and Johnson, P. F. (1991) *Genes Dev.* **5**, 1553–1567
- Jenkins, L. M., Yamaguchi, H., Hayashi, R., Cherry, S., Tropea, J. E., Miller, M., Wlodawer, A., Appella, E., and Mazur, S. J. (2009) *Biochemistry* **48**, 1244–1255
- Rost, B. (1996) *Methods Enzymol.* **266**, 525–539
- Rost, B., Yachdav, G., and Liu, J. (2004) *Nucleic Acids Res.* **32**, W321–326
- Gasteiger, E., Hoogland, C., Gattiker, A., Duvaud, S., Wilkins, M. R., Appel, R. D., and Bairoch, A. (2005) in *The Proteomics Protocols Handbook* (Walker, J. M., ed) pp. 571–607, Humana Press, Totowa, NJ
- Coeytaux, K., and Poupon, A. (2005) *Bioinformatics* **21**, 1891–1900
- Gaboriaud, C., Bissery, V., Benchetrit, T., and Mornon, J. P. (1987) *FEBS Lett.* **224**, 149–155
- Callebaut, I., Labesse, G., Durand, P., Poupon, A., Canard, L., Chomilier, J., Henrissat, B., and Mornon, J. P. (1997) *Cell Mol. Life Sci.* **53**, 621–645
- Choi, Y., Asada, S., and Uesugi, M. (2000) *J. Biol. Chem.* **275**, 15912–15916
- Tahirov, T. H., Sato, K., Ichikawa-Iwata, E., Sasaki, M., Inoue-Bungo, T., Shiina, M., Kimura, K., Takata, S., Fujikawa, A., Morii, H., Kumasaka, T., Yamamoto, M., Ishii, S., and Ogata, K. (2002) *Cell* **108**, 57–70
- He, B., and Wilson, E. M. (2003) *Mol. Cell Biol.* **23**, 2135–2150
- Trautwein, C., Walker, D. L., Plümpe, J., and Manns, M. P. (1995) *J. Biol. Chem.* **270**, 15130–15136
- Feng, H., Jenkins, L. M., Durell, S. R., Hayashi, R., Mazur, S. J., Cherry, S., Tropea, J. E., Miller, M., Wlodawer, A., Appella, E., and Bai, Y. (2009) *Structure* **17**, 202–210
- Wojciak, J. M., Martinez-Yamout, M. A., Dyson, H. J., and Wright, P. E. (2009) *EMBO J.* **28**, 948–958
- Joerger, A. C., and Fersht, A. R. (2008) *Annu. Rev. Biochem.* **77**, 557–582
- Mink, S., Haenig, B., and Klempnauer, K. H. (1997) *Mol. Cell Biol.* **17**, 6609–6617
- Nakajima, T., Kinoshita, S., Sasagawa, T., Sasaki, K., Naruto, M., Kishimoto, T., and Akira, S. (1993) *Proc. Natl. Acad. Sci. U.S.A.* **90**, 2207–2211
- Shuman, J. D., Vinson, C. R., and McKnight, S. L. (1990) *Science* **249**, 771–774
- Podust, L. M., Krezel, A. M., and Kim, Y. (2001) *J. Biol. Chem.* **276**, 505–513
- Fontes, M. R., Teh, T., and Kobe, B. (2000) *J. Mol. Biol.* **297**, 1183–1194
- Miller, M., Shuman, J. D., Sebastian, T., Dauter, Z., and Johnson, P. F. (2003) *J. Biol. Chem.* **278**, 15178–15184
- Burk, O., Mink, S., Ringwald, M., and Klempnauer, K. H. (1993) *EMBO J.* **12**, 2027–2038
- Burk, O., Worpenberg, S., Haenig, B., and Klempnauer, K. H. (1997) *EMBO J.* **16**, 1371–1380
- Ness, S. A., Kowenz-Leutz, E., Casini, T., Graf, T., and Leutz, A. (1993) *Gene Dev.* **7**, 749–759
- Gao, H., Parkin, S., Johnson, P. F., and Schwartz, R. C. (2002) *J. Biol. Chem.* **277**, 38827–38837
- Hu, H. M., Tian, Q., Baer, M., Spooner, C. J., Williams, S. C., Johnson, P. F., and Schwartz, R. C. (2000) *J. Biol. Chem.* **275**, 16373–16381
- Lee, Y. H., Williams, S. C., Baer, M., Sterneck, E., Gonzalez, F. J., and Johnson, P. F. (1997) *Mol. Cell Biol.* **17**, 2038–2047
- Spooner, C. J., Guo, X., Johnson, P. F., and Schwartz, R. C. (2007) *Mol. Immunol.* **44**, 1384–1392
- Zahnnow, C. A. (2009) *Expert. Rev. Mol. Med.* **11**, e12
- Nerlov, C., and Ziff, E. B. (1995) *EMBO J.* **14**, 4318–4328